VLA Scientific Memo 167:
Evaluation of C Array Single Configuration Imaging

M.A. Holdaway
National Radio Astronomy Observatory
Socorro, NM 87801

July 6, 1994

1 Abstract

The modified C configuration (CS) proposed by Braun (1993) for single configuration imaging of large objects has been evaluated with numerical simulations. We have explored the imaging fidelity for the CS, C alone, and C+D arrays together as a function of source size and observation hour angle range. We find that maximum entropy is far superior to CLEAN when imaging large objects. Generally, C+D arrays together results in the best imaging, followed by the CS array, and finally C array alone results in the poorest imaging. For intermediate source sizes the CS array's imaging quality approaches the C+D quality while far surpassing the C array's imaging, indicating that there are observations for which the CS array would be advantageous. However, as the length of the observations is increased to full tracks, all arrays perform equally well.

2 Introduction

Because the VLA configurations were not designed to give good single configuration imaging, large, complicated objects require observations in multiple array configurations if high resolution imaging is required. In VLA Scientific Memo 165, *Telescope Placement at the VLA for Better Single Configuration Imaging*, Robert Braun enumerates some of the problems with multiconfiguration observations and suggests new alternative C, B, and A configurations which contain more short spacings (referred to here as CS, BS, and AS, where S stands for *short spacings*). The extra short spacings in these alternative configurations are obtained by moving one (for CS) or three (for BS and AS) antennas from the outermost stations to more central stations, achieving improved configurations whithout any new construction, but at a small cost to resolution.

Adding new configurations to the VLA schedule is a major change to the routine array operations and needs to be explored carefully. In this document, I use numerical simulations in the SDE software package to examine the imaging characteristics of the CS array in comparison to the C array alone and the C and D arrays together.

3 Single Pointing Simulations

I chose the spectacular 1.4 GHz VLA image of Cassiopeia A (Braun, Gull, and Perley, 1987; see Figure 1) for the model brightness distribution. This image has lots of structure on many different scales, and is a good test of the imaging capabilities of the alternative arrays. For these simulations, the Cas A image was spatially scaled in powers of $\sqrt{2}$ from $5'$to $28'$. Simulations were performed for 1.4 GHz, $\delta = 20°$ with the C+D arrays (D array observations are taken to be 0.1 times the length of the C array observations), CS array, and C array for hour angle range of ± 0.5, ± 2.0, and ± 7.0 hours. One (u, v) point was calculated for each baseline every 5 minutes. No noise or other errors were added to the data. The effects of the primary beam have not been taken into account in either the simulations or the reconstructions. The data were gridded with uniform weight and Fourier transformed, and the dirty images were deconvolved with maximum entropy (Cornwell and Evans, 1985) and CLEAN (Clark, 1980). I have based most of my conclusions on images made with maximum entropy, but maximum entropy yields positive-biased images in the presence of noise. Future simulations should include thermal noise to understand imaging of weak sources.

Image reconstruction is evaluated by the fraction of the flux which is recovered, by the image fidelity, which is a measure of the *on source* signal to noise (Cornwell *et al.*, 1993), and by the distribution of errors in the (u, v) plane.

A plot for each hour angle simulation set shows the fraction of flux recovered for each configuration as a function of source size (Figures 2a through 2c). The entire flux is recovered for objects smaller than some critical size. The critical size depends upon the configuration and the hour angle range. The critical size increases with hour angle coverage. Quite surprisingly, most of the flux can be recovered for $28'$ objects, even with the C array alone, when observations are carried out to ± 7.0 hours (this is due to projected baselines at the limits of the observation and is likely to depend upon source declination). Critical size is smallest for the C array ($< 5'$ for ± 2 hour tracks), larger for the CS array ($\simeq 14'$ for ± 2 hour tracks), and largest for the combined C/D arrays ($> 14'$ for ± 2 hour tracks). The critical size is likely to depend upon source structure as well. The recovered flux decreases with object size for objects larger than the critical size.

In addition to the flux obtained from the maximum entropy deconvolution, the flux obtained from the best clean image (clean components plus residuals) is also displayed for a few simulation points. As can be seen, the clean flux is significantly lower than the flux given by maximum entropy.

The image fidelity is displayed for each hour angle simulation set shows the quality of each configuration's reconstruction as a function of source size (Figures 3a through 3c). A fidelity of 20 indicates that there is typically a 5% error in a pixel's flux, though there will be wild fluctuations in the pixel error across the image. The fidelity is typically much lower than the dynamic range, which measures off source errors. There is no critical size for the fidelity, but the fidelity should improve as the source structure becomes simpler (ie, as the source size decreases). Again, the C+D array typically produces better images than the CS array, and the CS array does better than the C array alone. An exception to this rule is the ± 7 hour

array	flux recovered	fidelity
C+D	0.638	2.5
CS	0.593	2.5
C	0.366	1.5

Table 1: Imaging performance of the C+D, CS, and C configurations for a mosaic observation with no total power added.

simulations, in which the CS array does not perform quite as well as the C array. This is not understood.

Figure 4 shows the residual visibility plots (fractional error as a function of radial (u, v) distance) for the C+D CLEAN deconvolution and the C+D, C, and CS configurations with MEM deconvolution for the 14′, ±2 hour simulations. A few interesting comparisons:

- poor reconstruction of source structure on the shortest spacings results in errors on all spacings.
- the C array MEM reconstruction is comparable to or somewhat better than the C+D CLEAN reconstruction.
- even though both C+D and CS MEM images recovered all of the flux, the error level is higher in the CS image (the CS fidelity is also lower than the C+D fidelity in Figure 3b).
- the CS image is far superior to the C image.

4 Mosaic Simulations

The CS configuration does a pretty good job at imaging large objects in single pointing observations. Mosaics using both C and D configurations are becoming more common: can the CS configuration make good mosaic images? Effective mosaicing depends strongly on good short spacing (u, v) coverage. I have simulated a 9 pointing mosaic with ±4 hours coverage with the C+D arrays (full time in D array now), the CS array, and the C array. The full D array tracks are usually justified for mosaicing on source-complexity grounds rather than signal-to-noise grounds.

Each pointing is reobserved every 25 minutes. No total power data is measured, and no noise or errors are added to the simulated data. The flux recovered and the fidelity are are shown in Table 1. Both quantities are mainly limited by the lack of total power data. The CS configuration did nearly as well as the C+D observations

5 Conclusions

From these simulations, it is clear that there are situations in which the CS array greatly outperforms the C array, but that the C+D option is still generally superior. Astronomers may find that the CS array is good enough for their observations. Simulations with thermal noise will be required to better understand the utility of the CS array, which would spend much of its time observing low SNR spectral line sources.

Simulations are also required to evaluate the BS and AS arrays. The BS and AS arrays may prove to be worthwhile for imaging objects which are larger than the standard B and A arrays can image, but I suppose that they would have difficulty imaging objects as large as can be imaged with the D array.

Looking at the radial profile of the (u, v) sampling density for a standard VLA array, there are many more short spacings than long; the (u, v) sampling density is $\sim$100 times higher in the most densely sampled region of the inner (u, v) plane than at 2/3 the maximum baseline. Instead of moving a few antennas from the ends of the arms, why not make the more radical move and ask what configuration, given existing antenna locations, produces the (u, v) coverage which is closest to what we really want?

6 References

1. Braun, Gull, and Perley, 1987, *Nature*, **327**, 395.
2. Braun, R., 1993, VLA Scientific Memo 165, *Telescope Placement at the VLA for Better Single Configuration Imaging.*
3. Clark, B.G., 1980, *Astron. Astrophys.*, **89**, 377-378.
4. Cornwell, T.J., and Evans, K.F., 1985, *Astron. Astrophys.*, **143**, 77-83.
5. Cornwell, T.J., Holdaway, M.A., and Uson, J.M., 1993, *Astron. Astrophys.*, **271**, 697-713.

Figure 1: Cassiopeia A was used as the model brightness distribution for these simulations.

Figure 2: How much flux can the VLA recover as a function of source size? Fraction of flux recovered in simulated observations for (a) C, CS, and C+D configurations with HA range = ± 0.5 hours, (b) ± 2.0 hours, and (c) ± 7.0 hours.

Figure 3: What quality image can the VLA produce as a function of source size? Image fidelity in simulated observations for (a) C, CS, and C+D configurations with HA range = ± 0.5 hours, (b) ± 2.0 hours, and (c) ± 7.0 hours.

Figure 4: Where are the errors in the Fourier plane? For the $14'$, ± 2.0 hour simulations, the fractional error in the Fourier plane is plotted as a function of radial (u, v) distance for (a) the C+D CLEAN reconstruction, (b) the C+D MEM reconstruction, (c) the C MEM reconstruction, and (d) the CS MEM reconstruction.

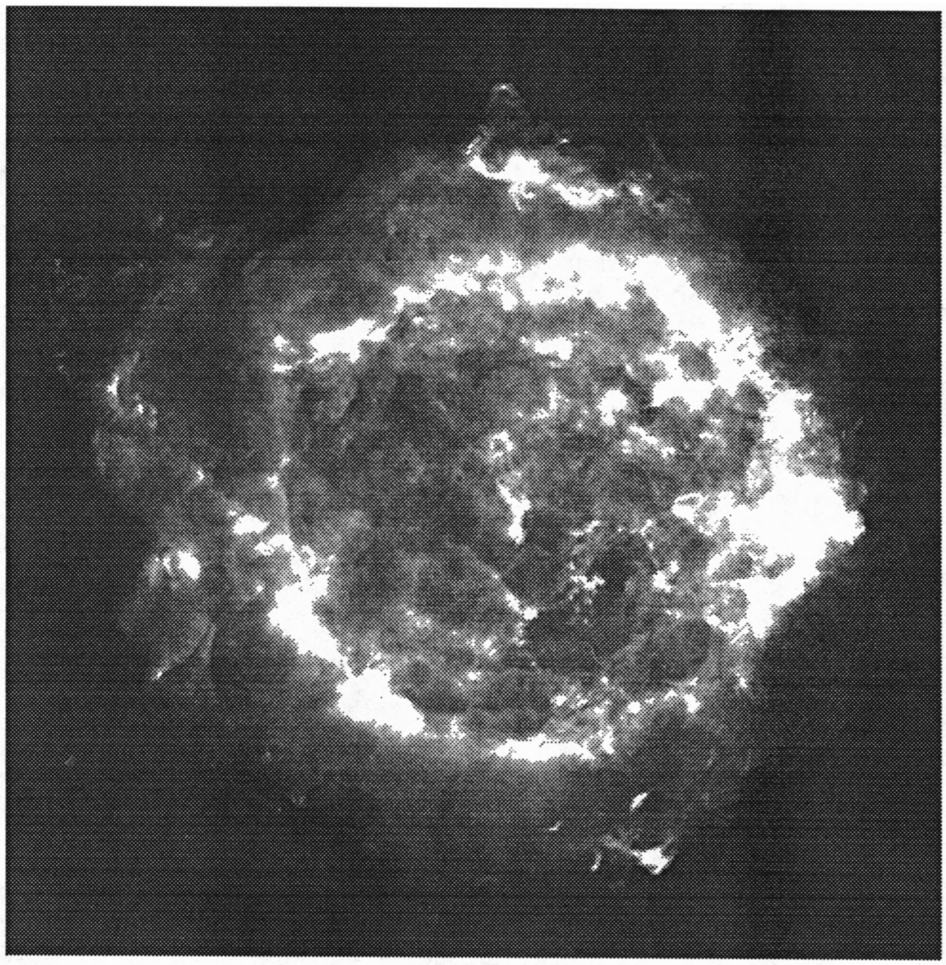

Figure 1

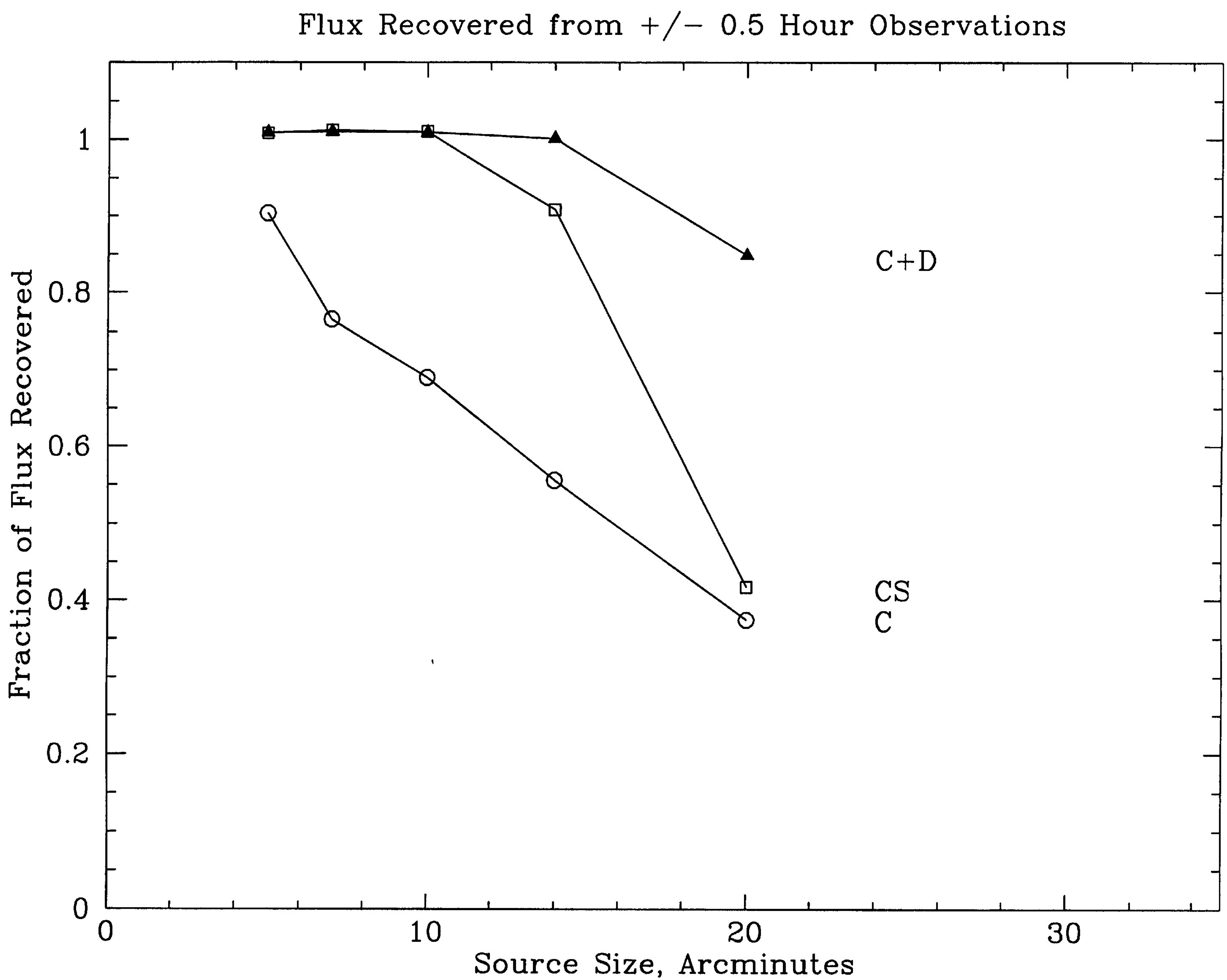
Flux Recovered from +/− 0.5 Hour Observations
Fraction of Flux Recovered
Source Size, Arcminutes
C+D
CS
C
0
0.2
0.4
0.6
0.8
1
10
20
30

Figure 2a

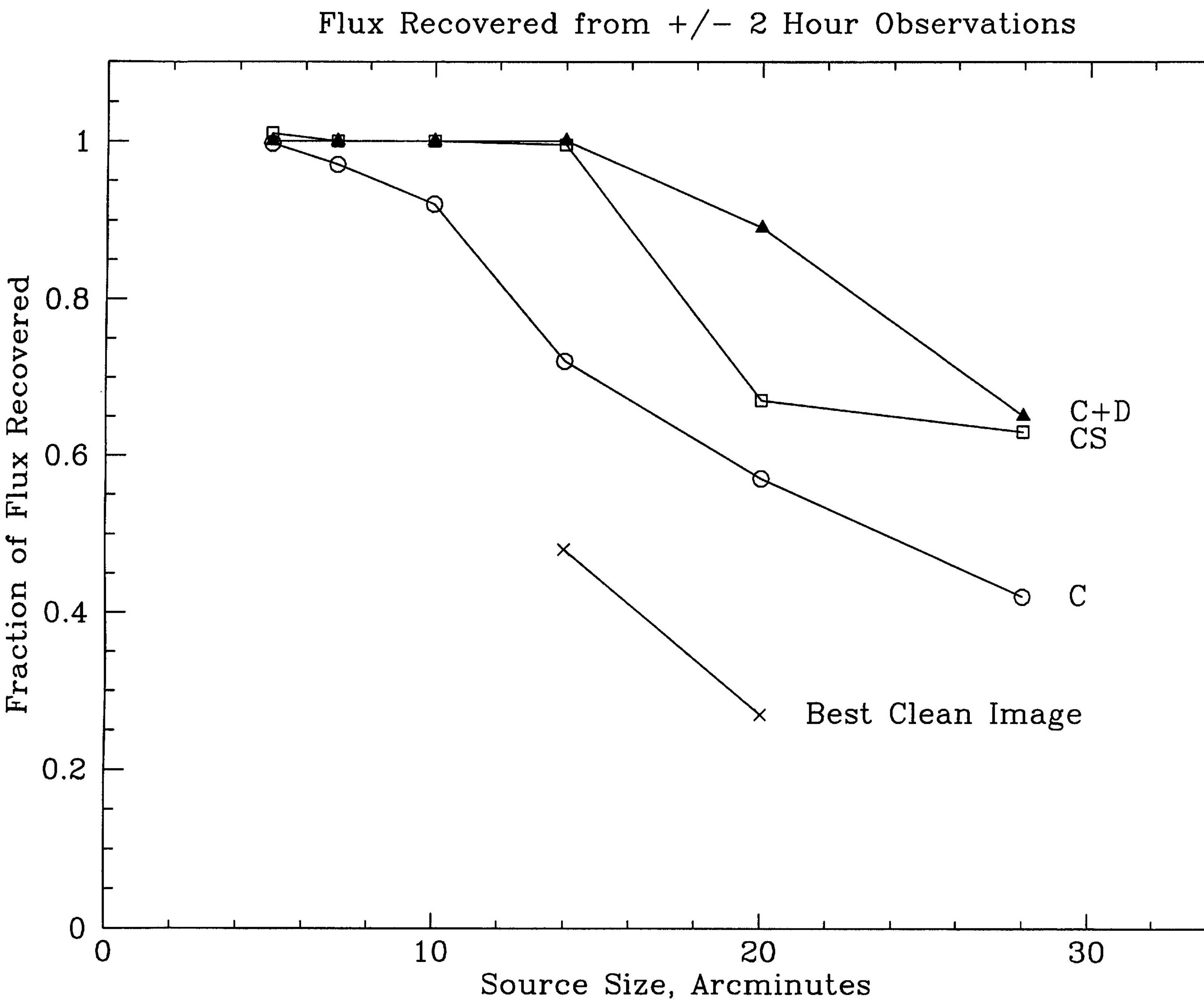

Flux Recovered from +/- 2 Hour Observations
Fraction of Flux Recovered
Source Size, Arcminutes
0
0.2
0.4
0.6
0.8
1
0
10
20
30
C+D
CS
C
Best Clean Image

Figure 2b

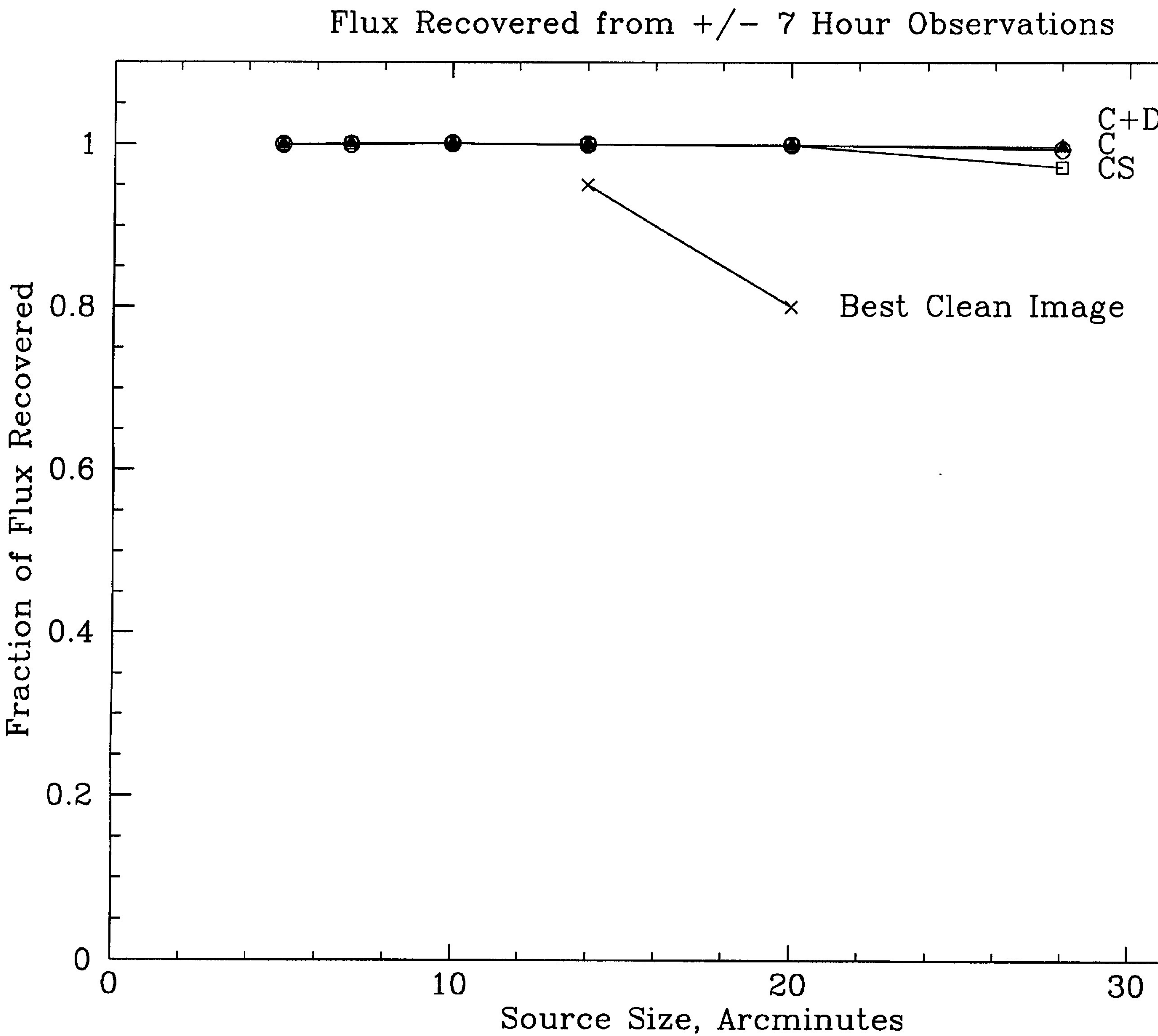
Flux Recovered from +/- 7 Hour Observations
Fraction of Flux Recovered
Source Size, Arcminutes
C+D
C
CS
Best Clean Image
0
0.2
0.4
0.6
0.8
1
0
10
20
30

Figure 2c

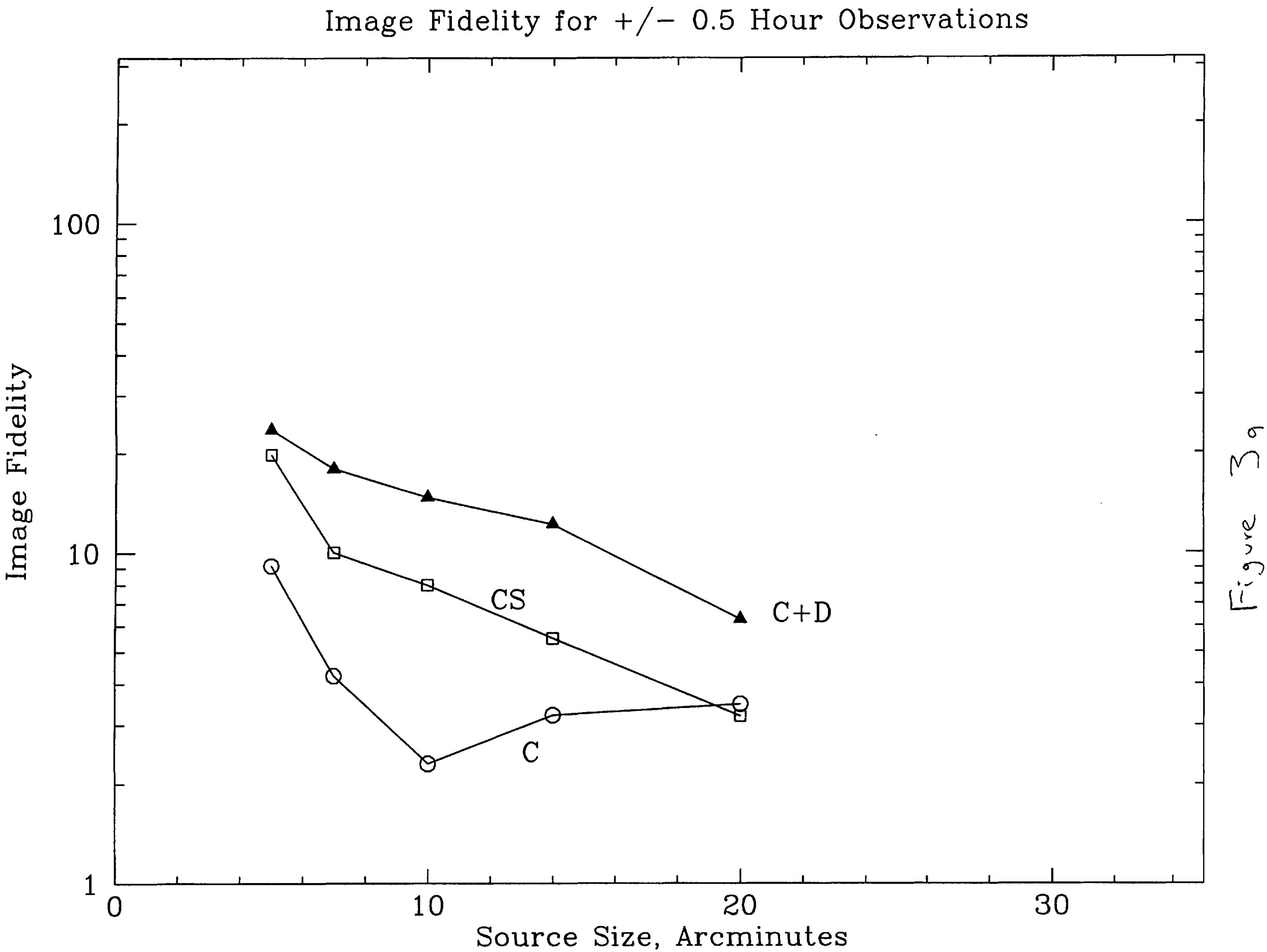
Image Fidelity for +/- 0.5 Hour Observations
Image Fidelity
100
10
1
0
10
20
30
Source Size, Arcminutes
C+D
CS
C
Figure 3a

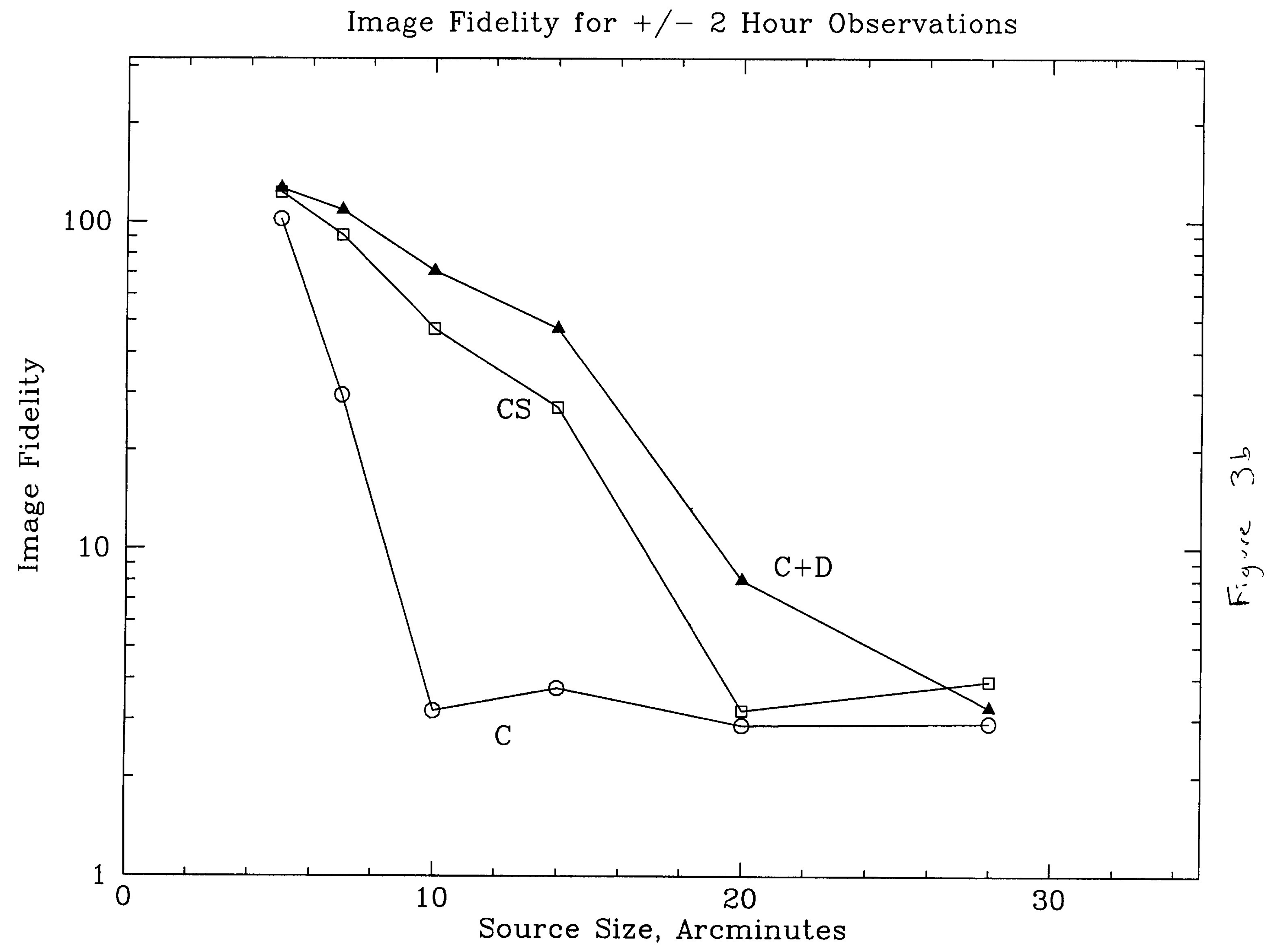
Image Fidelity for +/− 2 Hour Observations
Image Fidelity
Source Size, Arcminutes
100
10
1
0
10
20
30
CS
C+D
C
Figure 3b

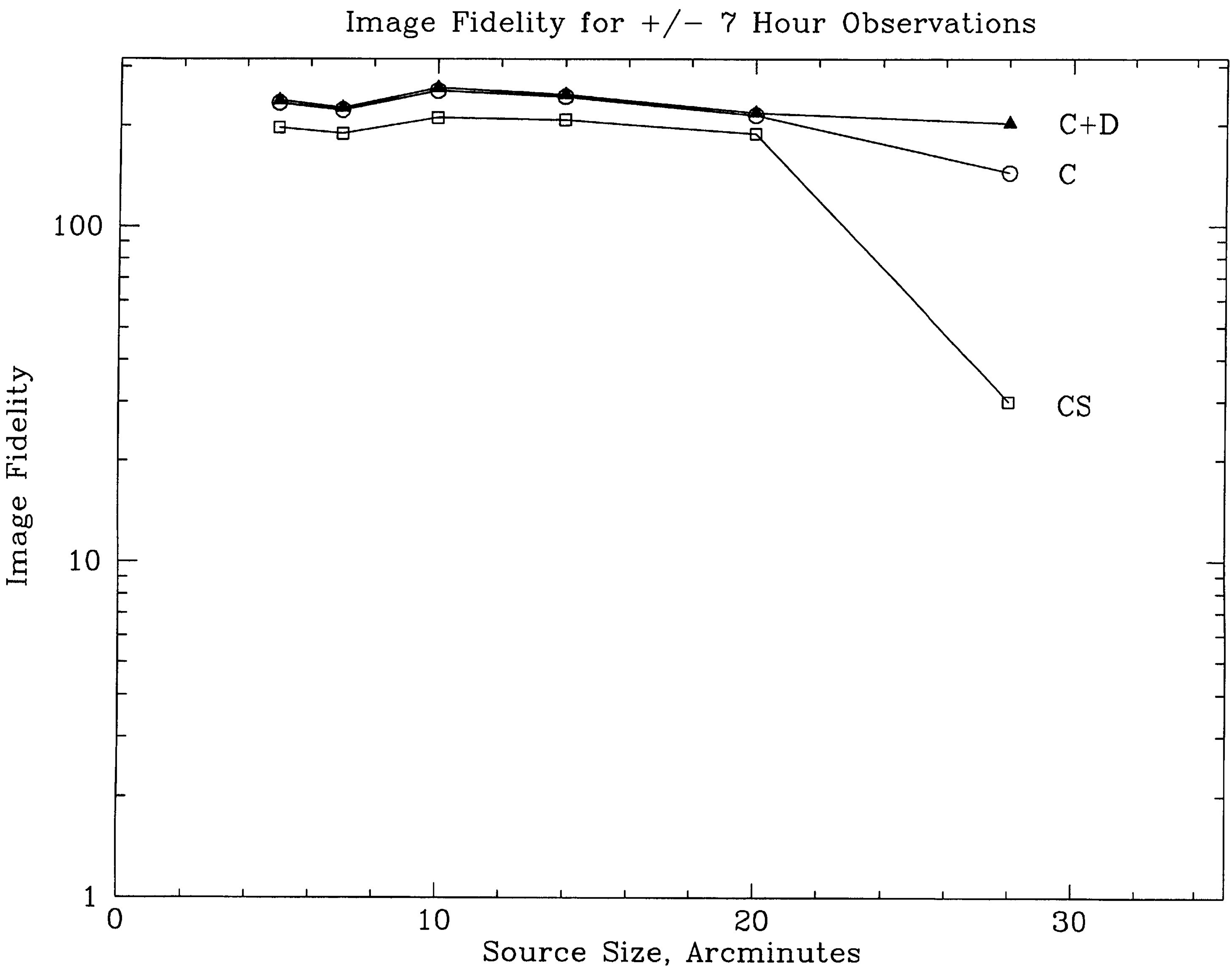

Image Fidelity for +/- 7 Hour Observations
Image Fidelity
Source Size, Arcminutes
1
10
100
0
10
20
30
C+D
C
CS

Figure 3c

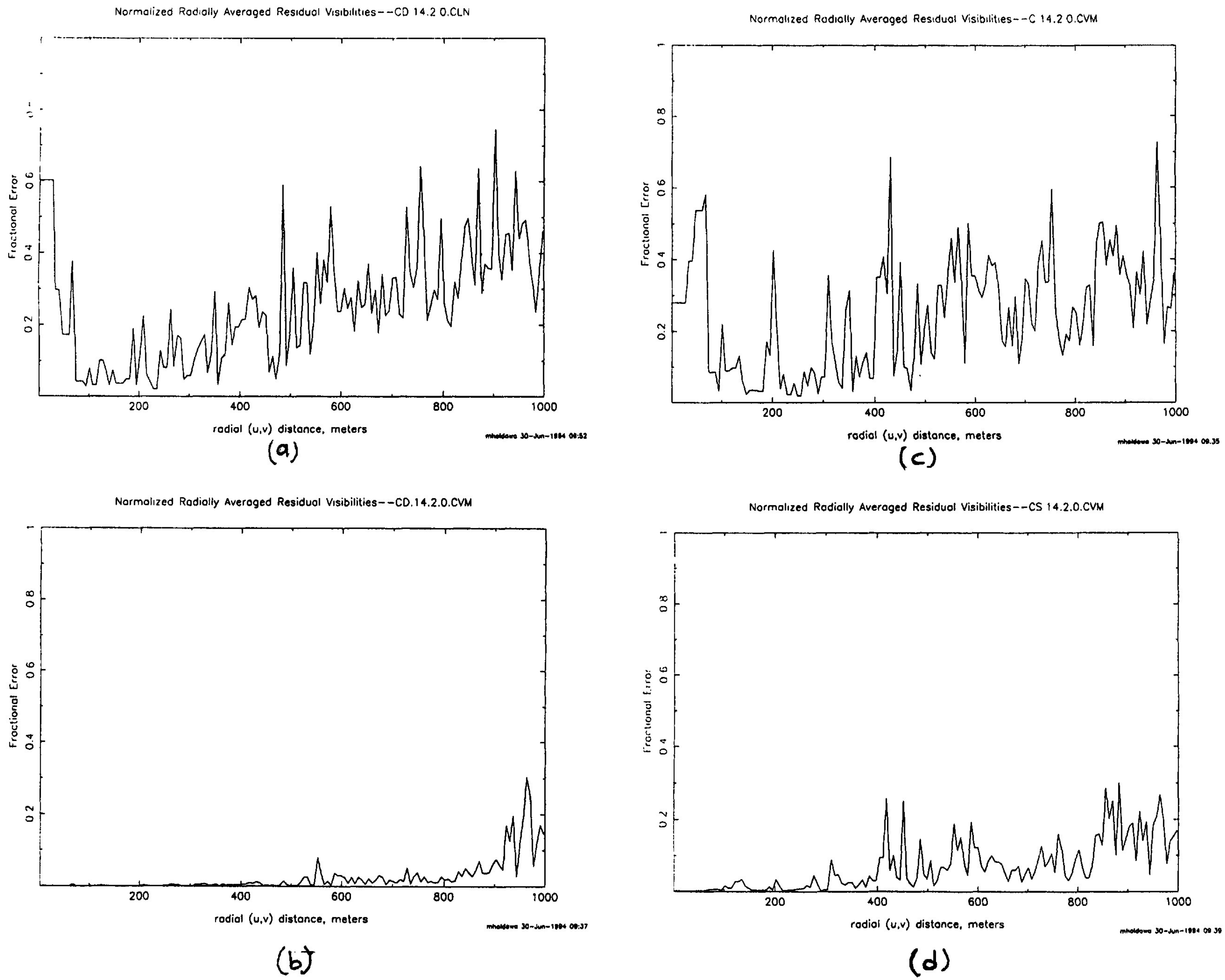
Normalized Radially Averaged Residual Visibilities--CD 14.2 0.CLN
Fractional Error
radial (u,v) distance, meters
(a)
Normalized Radially Averaged Residual Visibilities--CD.14.2.0.CVM
Fractional Error
radial (u,v) distance, meters
(b)
Normalized Radially Averaged Residual Visibilities--C 14.2 0.CVM
Fractional Error
radial (u,v) distance, meters
(c)
Normalized Radially Averaged Residual Visibilities--CS 14.2.0.CVM
radial (u,v) distance, meters
(d)

Figure A